Seakeeping optimization of a fast displacement catamaran on the basis of strip-theory codes

Filipe Belga

filipe.rbelga@gmail.com

Técnico Lisboa, Universidade de Lisboa, Portugal

December 2017

Abstract

The present work optimizes the seakeeping performance of a displacement catamaran in head seas to operate as a fast crew supplier for an offshore platform at the Alentejo basin, Portugal. In order to assess the accuracy in predicting heave and pitch motions of fast displacement catamarans (assuming negligible interaction between demi-hulls in head seas), three codes based on the ordinary strip-method were compared: the open-source code PDStrip, an in-house code earlier developed at CENTEC in Técnico Lisboa (IST) and the commercial software Maxsurf. The codes were applied to a fast catamaran and a fast mono-hull, for which experimental data from model testing were available. Results indicated PDStrip (with transom terms) as the most suited to be used in the optimization procedure. The RMS vertical acceleration responses at the bow and the average Motion Sickness Incidence (MSI) at the passenger area were selected as objective functions to minimize. Extreme effects such as slamming and green water were neglected, even though they might occur. As an attempt to include a preliminary design of the general arrangement, the dimensions and position of the passenger area on deck were set in order to minimize motion sickness. Stability criteria from the High Speed Craft (HSC) Code were applied, as well as a constraint on the maximum total ship resistance, computed with empirical formulae that estimate the hull interference components. Slender-body theory was used to calculate wave resistance. The effects of horizontal clearance ratios S/LWL between 0.2 and 0.4 were studied with respect to resistance, stability and MSI. The method of Lackenby was used to generate hull variations from a parent model, for which combinations of LCB and C_b were imposed, varied within the range of +-10%. Finally, an operability assessment of the optimized catamaran operating at two different speeds was carried out based on limiting seakeeping criteria imposed by the HSC Code and DNV-GL in terms of the average 1% highest accelerations.

Keywords: catamaran, strip theory, PDStrip, seakeeping optimization, RMS accelerations, motion sickness, Alentejo basin

1. Introduction

Despite a continuous misuse of fossil fuels, which has been contributing to serious environmental problems, the ever increasing rate of energy consumption still makes us highly dependent. In Portugal there has been a lot of speculation regarding the existence of economically viable reservoirs (e.g., [31]). In this regard, Carvalho (2016) conceptualized a potential deep offshore hydrocarbon field located 50 km off the coast of Sines, at the Alentejo basin. This work was the basis of the case study addressed in this dissertation, in which a fast displacement catamaran is used to supply crew to the offshore platform. As a high speed vessel, the requirement to operate well at high speeds, often in adverse weather conditions, is paramount and thus, the main emphasis was put into improving its seakeeping performance. Only heave and pitch motions in head seas were considered, as it represents the most critical situation for a catamaran, which is particularly stable transverse wise. Despite a definite shift to 3-D seakeeping codes observed nowadays, strip theories remain a meaningful research topic due their reasonable accuracy, particularly in predicting heave and pitch motions, the low computational power required and the fast calculations provided, even considering their limited range of applications (slow speeds, slender hulls, small motion amplitudes, inviscid fluid assumptions). They are particularly useful within academic contexts, during early design stages and for inclusion into optimization procedures as is the case here.

During the 1960's and 1970's, strip-theory based methods were widely developed, particularly in the frequency domain. The formulation of Salvesen et al. (1970) became a standard reference, being commonly cited even today. In order to consider effects that result in non-linear forces such as large amplitude motions, time-domain formulations were developed as well (e.g., [34], [17]). Other solutions, the so-called 2 1/2-D strip theories, attempted to add speed related effects into the hydrodynamic problem, an approach that lies somewhere between standard 2-D strip theories and 3-D panel methods (e.g., [15], [25]). To overcome the same limitations that motivated the development of strip theories in the time-domain, there was an increasing focus on 3-D panel methods, mainly via Rankine sources or Green function, both in time and frequency-domain, driven by the breakthroughs in computer sciences (e.g., [3], [10], [45]). Nowadays, the development of more complex, far more powerful, methods such as CFD solvers, particularly 3-D turbulence models like RANS, stand as the state of the art of the industry (e.g., [33], [8], [46]).

As for the application of strip theories to multi-hulls, several authors tried to include viscous considerations associated with the 3-D hydrodynamic interaction between the hull struts of SWATH vessels (e.g., [36], [30]). Attempts to extend these ideas to conventional catamaran hull forms have been made as well (e.g., [9], [47]). In any case, such effects are generally considered unimportant to the heaving and pitching of catamarans in head seas ([40], [23]).

Up until the late 1980's, despite the significant volume of research on hydrodynamic optimization of ship designs that included seakeeping considerations, the conclusions did not bear substantial developments ([41], [29]), as the bulk of the work would mainly focus on ship resistance (e.g., [39], [37]). With the widespread development of high-speed vessels and its use to transport passengers, light was shed upon the rel-

evance of seakeeping behaviour as hydrodynamic parameter to optimize. As stated before, the speed provided by strip methods is especially valuable when the seakeeping tool is to be embedded within optimization routines. Thus, they have been recurrently used, for instance, to assess the sensitivity of certain seakeeping characteristics of a vessel (e.g., heave/pitch RAOs, vertical accelerations, relative motions, slamming) upon the variation of the main particulars, which is often carried out with the intent of improving existing designs. Such studies commonly resort to systematic variations of the hull form parameters or main dimensions, as it is a quick and easy way to generate geometries from a parent model (e.g., [29], [42], [38]). Alternatively, parametric relationships can be set resorting, for instance, to polynomials (e.g., [28], [2]). Again, the development of more advanced and demanding 3-D numerical tools and their inclusion into routines to optimize both the seakeeping performance and ship resistance is, today, a common trend (e.g., [1], [48]).

Welfare and comfort are, especially for passenger ships, two very important aspects. From this perspective, several authors have evaluated seakeeping criteria with respect to motion sickness and habitability on-board, some of which focused on the influence of changes in hull geometry on such parameters (e.g., [42], [38]).

Considerations in terms of resistance, stability, etc., can be integrated either in the form of constraints to the seakeeping optimization problem (e.g., [29], [14]) or taken into account in a final stage where the hull with optimum seakeeping qualities is further refined with respect to those characteristics (e.g., [20]).

2. Benchmarking study of strip-theory codes to predict heave and pitch motions of fast displacement catamarans in head seas

2.1. *General formulation of equations of motion*

The equations of motion are presented here for a ship advancing with constant mean forward speed U in head seas in regular sinusoidal waves. In this section, based on the frequency domain formulation of Salvesen et al. (1970), only the global governing equations will be presented. For a more extensive reading, Fonseca (2009) presents a thorough review of the complete hydrodynamic problem within ideal fluid assumptions, including the derivation of the boundary value problem and its linearisation.

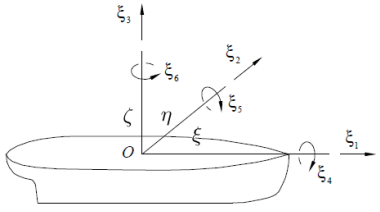

Figure 1: General reference frame and motion conventions ([16], adapted)

Let (ξ, η, ζ) be the fixed inertial reference frame with respect to the mean position of the ship in steady translation with the forward velocity U, with ζ vertically upwards through the centre of gravity, ξ in the direction of forward motion and at the origin of the undisturbed free surface as seen in Figure 1. Ship motions comprise three translatory displacements - surge (ξ_1), sway (ξ_2) and heave (ξ_3) - and three angular displacements - roll (ξ_4), pitch (ξ_5) and yaw (ξ_6).

For a ship with lateral symmetry and slender hull form, under the assumptions that the responses are linear and harmonic, the derived equations for coupled heave and pitch motions can be written in matrix form as follows:

$$\begin{bmatrix} \Delta + A_{33} & A_{35} \\ A_{53} & I_{55} + A_{55} \end{bmatrix} \begin{Bmatrix} \ddot{\xi}_3 \\ \ddot{\xi}_5 \end{Bmatrix} + \begin{bmatrix} B_{33} & B_{35} \\ B_{53} & B_{55} \end{bmatrix} \begin{Bmatrix} \dot{\xi}_3 \\ \dot{\xi}_5 \end{Bmatrix} + \begin{bmatrix} C_{33} & C_{35} \\ C_{53} & C_{55} \end{bmatrix} \begin{Bmatrix} \xi_3 \\ \xi_5 \end{Bmatrix} = \begin{Bmatrix} \left|F_3^E\right| \\ \left|F_5^E\right| \end{Bmatrix} e^{i\omega_e t} \tag{1}$$

, where for $j, k = 3, 5$, A_{jk} and B_{jk} are the added mass and damping coefficients computed as in Table 1, C_{jk} are the hydrostatic restoring coefficients as given by equations (2) and $\left|F_j^E\right|$ are the complex amplitudes of the exciting force/moment $F_j^E = \left|F_j^E\right| e^{i\omega t}$ as presented in Table 2. t stands for the time variable, Δ represents the total mass of the ship and I_{55} is the moment of inertia in the 5^{th} mode. The frequency of encounter ω_e is the same as the frequency of the response and relates to the wave frequency ω_0 by $\omega_e = \omega_0 - k_0 U \cos\beta$. $k_0 = \omega_0^2/g$ is the wave number, g is the acceleration of gravity and β is defined as the ship heading relative to the waves, for which the convention used here assumes $\beta = 180°$ for head seas.

Table 1: Added mass and damping coefficients for heave/pitch coupled motions [40]

	Original	Transom corrections
A_{33}	$\int_L a_{33} d\xi$	$-\frac{U}{\omega_e^2} b_{33}^{tr}$
B_{33}	$\int_L b_{33} d\xi$	$+U a_{33}^{tr}$
A_{35}	$-\int_L \xi a_{33} d\xi - \frac{U}{\omega_e^2} B_{33}^0$	$+\frac{U}{\omega_e^2} x_{tr} b_{33}^{tr} - \frac{U^2}{\omega_e^2} a_{33}^{tr}$
B_{35}	$-\int_L \xi b_{33} d\xi + U A_{33}^0$	$-U x_{tr} a_{33}^{tr} - \frac{U^2}{\omega_e^2} b_{33}^{tr}$
A_{53}	$-\int_L \xi a_{33} d\xi + \frac{U}{\omega_e^2} B_{33}^0$	$+\frac{U}{\omega_e^2} x_{tr} b_{33}^{tr}$
B_{53}	$-\int_L \xi b_{33} d\xi - U A_{33}^0$	$-U x_{tr} a_{33}^{tr}$
A_{55}	$\int_L \xi^2 a_{33} d\xi + \frac{U^2}{\omega_e^2} A_{33}^0$	$-\frac{U}{\omega_e^2} x_{tr}^2 b_{33}^{tr} + \frac{U^2}{\omega_e^2} x_{tr} a_{33}^{tr}$
B_{55}	$\int_L \xi^2 b_{33} d\xi + \frac{U^2}{\omega_e^2} B_{33}^0$	$+U x_{tr}^2 a_{33}^{tr} + \frac{U^2}{\omega_e^2} x_{tr} b_{33}^{tr}$

Table 2: Heave exciting force and pitch exciting moment [40]

	Original	Transom corrections
F_3^E	$\rho\xi_a \int_L \left(f_3^D + f_3^K\right) d\xi$	$+\rho\xi_a \frac{U}{i\omega_e} f_3^{D^{tr}}$
F_5^E	$-\rho\xi_a \int_L \left[\xi \left(f_3^D + f_3^K\right) + \frac{U}{i\omega_e} f_3^D\right] d\xi$	$-\rho\xi_a \frac{U}{i\omega_e} x_{tr} f_3^{D^{tr}}$

$$\begin{aligned} C_{33} &= \rho g A_{wp} \\ C_{35} &= C_{53} = -\rho g M_{yy} \\ C_{55} &= \rho g \nabla G M_L \end{aligned} \tag{2}$$

Here, all the integrals are along the length of the ship L. a_{33} and b_{33} represent the sectional added mass and damping coefficients in ζ direction. A_{33}^0 and B_{33}^0 refer to the speed independent components of A_{33} and B_{33}. x_{tr} is the $\xi-$coordinate of the aftermost cross section of the ship and a_{33}^{tr} and b_{33}^{tr} are the added mass and damping coefficients evaluated at that section. f_3^K and f_3^D represent, respectively, the sectional Froude-Krylov and diffraction forces in the vertical direction ($\zeta-$ axis) for unit amplitude incident waves. Regarding the former component, associated with the field of incident waves, the classical theory of linear gravity-waves defines, within deep water assumptions, the potential of a progressive incident wave with an arbitrary direction, which

makes f_3^K easy to compute by evaluating it at the mean wetted cross section. Alternatively, it can be computed at each time step, an approach commonly followed by time domain formulations. As for f_3^D, which measures the perturbation of the field of incident waves due to the presence of the ship, instead of determining directly the 2-D diffraction potential, Green theorem is usually applied in order to solve it as function of the 2-D radiation potential ([16], [40]). Finally, f_3^{Dtr} is the diffraction force evaluated at the aftermost section at x_{tr}. ξ_a represents the wave amplitude and ρ is the fluid density. Finally, ∇ is the static underwater hull volume, A_{wp} is the static waterplane area, M_{yy} is the first area moment of the static waterplane and GM_L the longitudinal metacentric height.

The solutions of the second order linear differential equations (1) are harmonic:

$$\xi_j(\omega_e) = \Re\{\xi_j^A e^{i\omega_e t}\} = \xi_j^a \cos(\omega_e t - \theta_j), \quad j = 3, 5 \tag{3}$$

, where ξ_j^A is the complex amplitude of the harmonic motion, ξ_j^a is the real amplitude and θ_j the phase angle that represents the delay of the response.

Finally, to express fixed coordinates of remote locations along the ship, a new reference frame (x, y, z) is here defined as the inertial reference frame (ξ, η, ζ) shifted along ξ to the aft perpendicular of the vessel. Following this notation, the absolute vertical displacement ξ_z at a remote location (x, y, z) is given by equation (4), assuming the motions are small. It is important to note that rolling motions are being neglected, i.e., vertical motions do not vary with y.

$$\xi_z(x, \omega_e) = \Re\{\left[\xi_3^A(\omega_e) - x\xi_5^A(\omega_e)\right] e^{i\omega_e t}\} \tag{4}$$

2.2. *Overview of Fonseca, PDStrip and Maxsurf Motions*

To select a seakeeping tool for the optimization of the crew supply catamaran, a benchmarking study of three available codes based on the ordinary strip-method of Salvesen et al. (1970) was carried out. Three software packages were considered, namely, PDStrip, an open-source code developed by Söding and Bertram (2009); Fonseca, an in-house code earlier developed at CENTEC in Técnico Lisboa (IST) (linear version of Fonseca and Guedes Soares, 1998) and the commercial software Maxsurf Motions [4]. Despite a few non-linear considerations by PDStrip, all the codes are linear and the computations are carried out in the frequency domain. Bellow, their main features are presented.

Table 3: Coordinate systems used by the codes

	Code	Coordinate Origin	+ x-axis	+ y-axis	+ z-axis
Geometry Data	Fonseca	fwdPP, centerplane, DWL	aft	Port	↑
	PDStrip	amidships, centerplane, baseline	fwd	Port	↑
	MaxMotions	non applicable	fwd	SB	↑
Inputs	Fonseca	amidships, centerplane, DWL	fwd	Port	↑
	PDStrip	amidships, centerplane, baseline	fwd	Port	↑
	MaxMotions	amidships, centerplane, baseline	fwd	SB	↑
Motion Results	Fonseca	LCG, centerplane, baseline	fwd	Port	↑
	PDStrip	amidships, centerplane, baseline	fwd	SB	↓
	MaxMotions	LCG, centerplane, baseline	fwd	SB	↑

Table 4: Main features of the codes

Features	Fonseca	PDStrip	MaxMotions
Non-linear motions	No	No	No
Non-linear transverse drag forces	No	Yes	No
Transom terms	No	Yes (optional)	Yes (optional)

Table 5: Methods applied by the codes to compute the radiation potential

Code	Method	Reference
Fonseca	Frank close-fit source distribution method	[19]
PDStrip	Patch method	[43]
MaxMotions	Multi-parameter conformal mapping	[4]

In any case, it is important to note that, despite a few variations, the three codes follow in a general sense the formulation presented in Section 2.1. For space economy, such details are neglected here. However, the author encourages reading the respective references stated in the first paragraph of the present section.

2.3. *Verification and validation with model tests of a fast mono-hull and a fast displacement catamaran*

The three codes were applied to two ship forms showed in Figure 2: the fast mono-hull Model5 [6] and a fast displacement river-going catamaran [22], for which experimental data from model testing was available. In the latter case, an assumption about negligible interaction between the hulls, which is acceptable in head and following seas, was exploited.

Table 6: Main dimensions of the full-scale vessels

	LWL [m]	BWL [m]	T [m]
Catamaran, demi-hull [22]	43	2.7	1.35
Model5 [6]	50	5.83	1.57

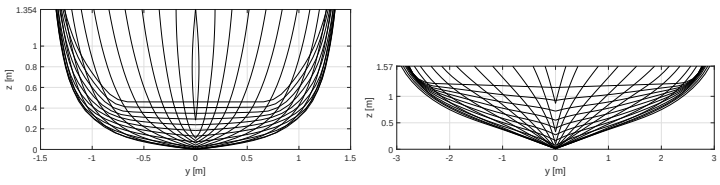

(a) Catamaran demi-hull [22] (b) Model5 [6]

Figure 2: Underwater body lines of the full-scale vessels

In the case of the catamaran, four Froude numbers ranging between 0 and 0.6 were analysed, while for Model5 only the Froude number values 0.57 and 1.14 have been considered. The peculiarity of the studied vessels is the high Froude numbers at which they were tested, which increases possible uncertainties caused by the strip method assumptions. Comparisons have been performed for the heave and pitch RAOs (Response Amplitude Operators) computed whenever possible both with and without transom terms activated.

These motion amplitudes are plotted versus wave frequency and each graph corresponds to a different Froude number. Results for the catamaran case can be seen in Figure 3

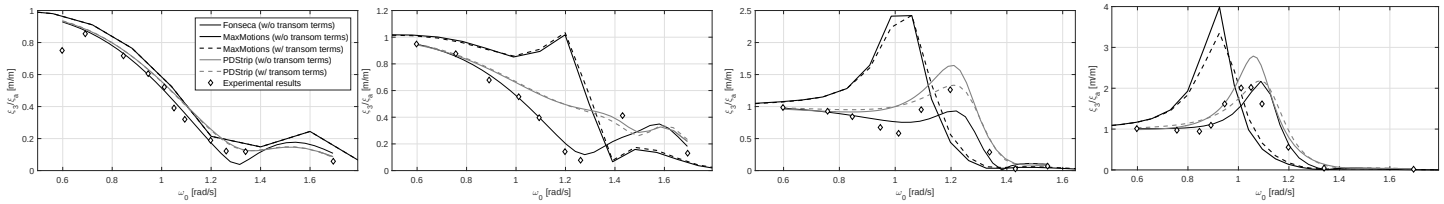

(a) Fn = 0 (b) Fn = 0.2 (c) Fn = 0.4 (d) Fn = 0.6

Figure 3: Heave RAOs as function of the wave frequency, Catamaran

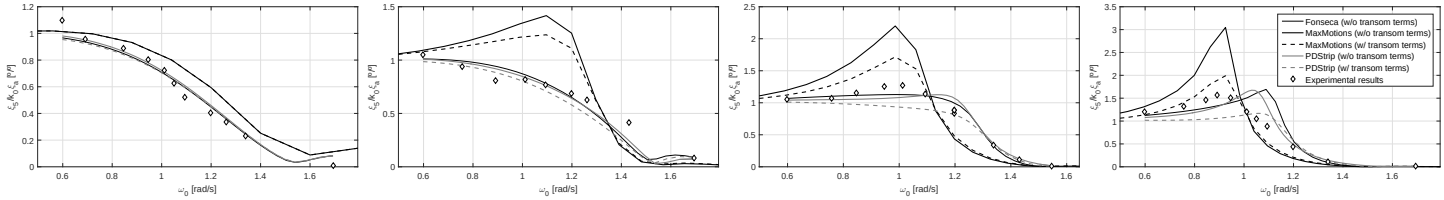

(a) Fn = 0 (b) Fn = 0.2 (c) Fn = 0.4 (d) Fn = 0.6

Figure 4: Pitch RAOs as function of the wave frequency, Catamaran

for heave and Figure 4 for pitch, while for Model 5 one should refer to Figure 5 for heave and Figure 6 for pitch. In each plot the numerical results can be compared with the corresponding data from model testing.

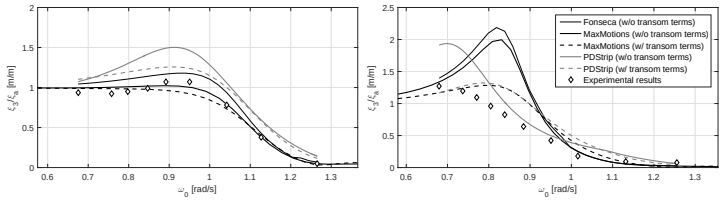

(a) Fn = 0.57 (b) Fn = 1.14

Figure 5: Heave RAOs as function of the wave frequency, Model5

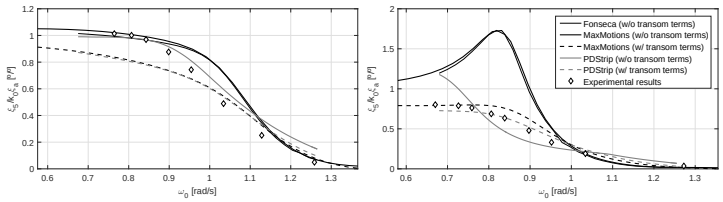

(a) Fn = 0.57 (b) Fn = 1.14

Figure 6: Pitch RAOs as function of the wave frequency, Model5

It can be observed that with increasing vessel speed, the accuracy in predicting heave and pitch motions with strip theory decreases, a well-known limitation of such theories and a general principle that must be taken into account. For the higher Froude numbers ($F_n = 0.6, 1.14$), heave and pitch response peaks are generally overestimated. Also, results indicate that the inclusion of transom terms damps the system, being generally beneficial for predicting heave and pitch motions, i.e., PDStrip and Maxsurf Motions with transom terms performed better. For $F_n = 0, 0.2, 0.4, 0.57$, not using transom terms is a better option, for which Fonseca seems to be the most suited choice. PDStrip, without transom terms, also performs reasonably well.

The order of magnitude of the differences between numerical and experimental results for the case of the fast mono-hull and the catamaran seems to indicate that all the studied codes perform better with the fast mono-hull. This was an expected result since these methods neglect phenomenon associated with hull interaction. In any case, PDStrip with transom terms seems reasonably accurate for heaving/pitching catamarans being capable of determining the resonance peak, both in terms of frequency and amplitude, with sufficient accuracy, particularly at higher speeds. In addition, PDStrip allows a large number of ship sections and offset points for geometry discretization, which improves accuracy during seakeeping computations, as well as a large number of wavelengths within a wide range to be used for motion results, being advantageous for a proper definition of the complete frequency spectrum. Also, from the perspective of embedding the code into an optimization procedure where a minimum level of automation is required, PDStrip can be conveniently compiled into an executable file with separate input text files. Finally, as an open source Fortran code, it is possible to edit and improve PDStrip if necessary, a useful characteristic bearing future work in mind.

3. Seakeeping optimization of a fast crew supplier catamaran to operate at the Alentejo basin

3.1. *Description of the parent model and seastates*

In order to base the optimization on a realistic parent vessel, the author contacted DAMEN Shipyards that provided the model of a 30 metre catamaran operating at a service speed of 25 knots and achieving a maximum of 30 knots. The number of passengers was set to 12, which, according to the HSC code [26], classes the vessel as a cargo craft.

The catamaran is here designed to operate at the Alentejo basin, transporting crew between shore and an offshore platform located 50 km off the coast of Sines. The discretization of the wave regime along the Portuguese coast has been done by Instituto Hidrográfico (Costa et al., 2001) and the measurements from Sines station were used to characterize the seastates at the Alentejo basin (Table 7).

Table 7: Scatter diagram [%] for the Alentejo basin, measured at Sines station between 1988-2000 [12]

$H_{1/3}$	T_p [s]								
[m]	3-5	5-7	7-9	9-11	11-13	13-15	15-17	>17	
0-1	0.480	1.210	2.620	6.760	6.790	3.520	1.350	0.110	*22.840*
1-2	1.020	2.590	5.600	14.450	14.510	7.530	2.880	0.230	*48.810*
2-3	0.390	0.990	2.140	5.530	5.550	2.880	1.100	0.090	*18.670*
3-4	0.140	0.360	0.780	2.020	2.030	1.050	0.400	0.030	*6.810*
4-5	0.040	0.110	0.240	0.610	0.610	0.320	0.120	0.010	*2.060*
5-6	0.020	0.040	0.090	0.240	0.240	0.120	0.050	0.000	*0.800*
	2.090	*5.300*	*11.470*	*29.610*	*29.730*	*15.420*	*5.900*	*0.470*	*100%*

The JONSWAP spectrum, extensively applied in the offshore industry, was selected as analytical model to represent the wave spectrum at the location. The formulation presented here [16], depends on the significant wave height $H_{1/3}$ and peak period T_p.

$$S_\zeta(\omega_0) = \frac{\alpha}{\omega_0^5} e^{-1.25\left(\frac{\omega_p}{\omega_0}\right)^4} \gamma^{e^{-\frac{1}{2\sigma^2}\left(\frac{\omega_0}{\omega_p}-1\right)^2}} \tag{5}$$

where,

$$\omega_p = \frac{2\pi}{T_p} \tag{6}$$

$$\alpha = 5\pi^4 (1 - 0.287 \log\gamma) \frac{H_{1/3}^2}{T_p^4} \tag{7}$$

$$\gamma = \begin{cases} 5, & \text{if} \quad T_p \leq 3.6\sqrt{H_{1/3}} \\ e^{5.75-1.15\left(\frac{T_p}{\sqrt{H_{1/3}}}\right)}, & \text{if} \quad 3.6\sqrt{H_{1/3}} < T_p \leq 5\sqrt{H_{1/3}} \\ 1, & \text{if} \quad T_p > 5\sqrt{H_{1/3}} \end{cases} \tag{8}$$

$$\sigma = \begin{cases} 0.07, & \text{if} \quad \omega_0 \leq \omega_p \\ 0.09, & \text{if} \quad \omega_0 > \omega_p \end{cases} \tag{9}$$

In order to account with the relative velocity between the ship and the encountering head waves, the sea spectrum $S_\zeta(\omega_e)$ is defined in equation (10). Finally, the basis to calculate vessel responses is the transfer function of that response. Considering equation (4) that expresses the transfer function of the absolute vertical displacement ξ_z at a remote location (x, y, z), the corresponding response spectrum S_z is given by equation (11):

$$S_\zeta(\omega_e) = \frac{S_\zeta(\omega_0)}{1 - \frac{2\omega_0 U}{g}} \tag{10}$$

$$S_z(x, \omega_e) = |\xi_z(x, \omega_e)|^2 S_\zeta(\omega_e) \tag{11}$$

3.2. *Overview of the optimization problem*

The flowchart in Figure 9 illustrates the procedure that automatically generates hull variations and evaluates the solutions in terms of seakeeping, resistance and stability, as well as all the numerical tools used for that purpose. Regarding the first aspect, it was used the method of Lackenby [5] to vary the block coefficient (C_b) and the longitudinal centre of buoyancy (LCB) both by +-10% of the parent values (in a total of 225 models evaluated) while maintaining the displacement (Δ), waterline length (LWL) and maximum beam at the waterline (BWL). Given the lack of information in terms of weight distribution at this early design stage, values for KG and LCG were assumed ($KG = 1.5$ meters from the baseline and $LCG = LCB$ for all generated models) which, in principle, should not affect the seakeeping characteristics of the vessel significantly [29]. Furthermore, it is important to note that not all generated models resulted into feasible solutions from the point of view of geometry. Not only excessively distorted models were discarded, as well as models not suited for numerical discretization by PDStrip which outputs warnings in such cases [44].

As for seakeeping assessment, in the present work, vertical accelerations, which are known to significantly decrease the operability level of high-speed vessels, were selected as parameter to minimize. In particular, RMS (Root Mean Squared) values are considered good statistical measures as they provide useful and immediate (although inevitably less detailed) information, without the need to consider the whole frequency spectrum. For the case of the acceleration responses, RMS_{a_z} are calculated as in equation (12).

$$RMS_{a_z}(x) = \sqrt{\int_{\omega_e} \omega_e^4 S_z(x, \omega_e)\, d\omega_e} \tag{12}$$

Thus, the minimization of maximum RMS_{a_z} value on deck, given the most probable seastate the vessel would have to face sailing at service speed was set as the main objective function of this optimization procedure. Logically, this corresponds to a location at the forward extremity of the vessel ($x = LOA$). In any case, given that LOA of the generated models might change, the author was forced to evaluate RMS_{a_z} at a fixed location near the bow, i.e., $x = 28.5$ metres, approximately at the same vertical of LWL, which is the same for all models. In addition, as an attempt to assess welfare and comfort of the crew on-board, motion sickness was computed and minimized as well. The time dependent MSI (Motion Sickness Incidence) model of McCauley et al. (1976) assess the percentage of passengers who vomit after a given time of exposure to a certain motion. This was very useful as the actual voyage time of the catamaran is known (65 minutes to sail 50 km at 25 knots) - Figure 7. Here, the formulation described in [11] is presented and depends on the average RMS_{a_z} and the average peak frequency f_e.

$$MSI = 100\Phi(z_a)\,\Phi(z_t) \tag{13}$$

, where $\Phi(z)$ is the standard normal distribution function.

$$\Phi(z) = \frac{1}{\sqrt{2\pi}} e^{-\frac{z^2}{2}} \tag{14}$$

$$z_a = 2.128 \log_{10}\left(\frac{|RMS_{a_z}|}{g}\right) - 9.277 \log_{10}|f_e| - 5.809 (\log_{10}|f_e|)^2 - 1.851 \tag{15}$$

$$z_t = 1.134 z_a + 1.989 \log_{10} t - 2.904 \tag{16}$$

$$|RMS_{a_z}| = 0.798 RMS_{a_z} \tag{17}$$

$$|f_e| = \frac{1}{2\pi} \frac{RMS_{a_z}}{RMS_{v_z}} \tag{18}$$

$$RMS_{v_z}(x) = \sqrt{\int_{\omega_e} \omega_e^2 S_z(x, \omega_e)\, d\omega_e} \tag{19}$$

The MSI was then computed at multiple locations at the area reserved to carry the passengers/crew. As an attempt to include a preliminary study of the general arrangement into the optimization procedure, the passenger area was positioned

on deck so that the average MSI was minimum. For this purpose, its position was fixed as illustrated in Figure 8 and the area needed to transport 12 passengers was estimated based on regresion analysis (48.24 m^2). It becomes now clear that for a constant passenger area with fixed width, its length and position will change according to the horizontal clearances ratio S/LWL that is being considered (a range between 0.2 and 0.4 was studied). Here, S refers to the distance between the centrelines of the demi-hulls.

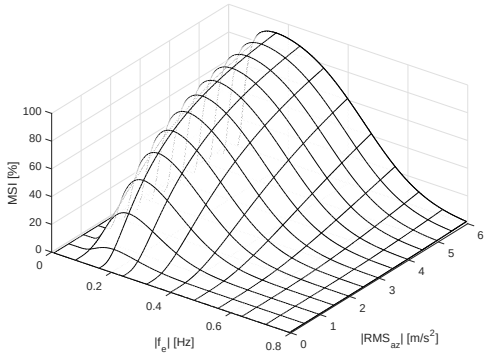

Figure 7: MSI model as proposed by [32], considering $t = 65$ min.

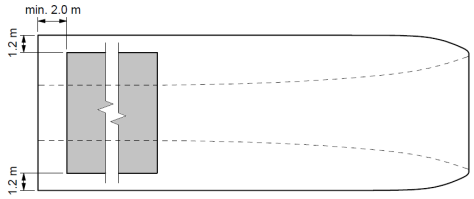

Figure 8: Position on deck of the passenger area (in grey) with respect to the ship sides and the aft perpendicular

In terms of constraints to the problem, the first has to do with total hull resistance and the second with stability requirements imposed by the HSC code [26]. Again, for space economy, a complete overview of each constraint will be skipped here. Generally speaking, the upper bound in terms of total ship resistance is imposed by the DAMEN catamaran with the original horizontal clearance, i.e., models with higher resistance values are discarded. To compute hull resistance, the methodology proposed in Jamaluddin et al. (2013) was used, which depends on an empirical formulae to calculate the interference of the ship resistance components dependent on the horizontal clearance ratio S/LWL that, as stated before, was varied between 0.2 and 0.4. The coefficient of friction resistance was obtained by the well known formula of ITTC-1957 and the wave-making resistance component was calculated with slender-body theory by the resistance package of Maxsurf [4]. Regarding stability, points 1.1 and 1.2 of *Annex 7 Stability of Multi-hull Craft, 1 Stability Criteria in the Intact Condition* from HSC code [26] were applied. Maxsurf Stability [5] was used to compute stability curves. It is important to note that for stability, in order to study horizontal clearances different than the parent value ($S/LWL = 0.2872$) each generated hull variation would have to be modelled individually with different S values prior to the stability analysis, which was not feasible. For this reason only $S/LWL = 0.2872$ was considered.

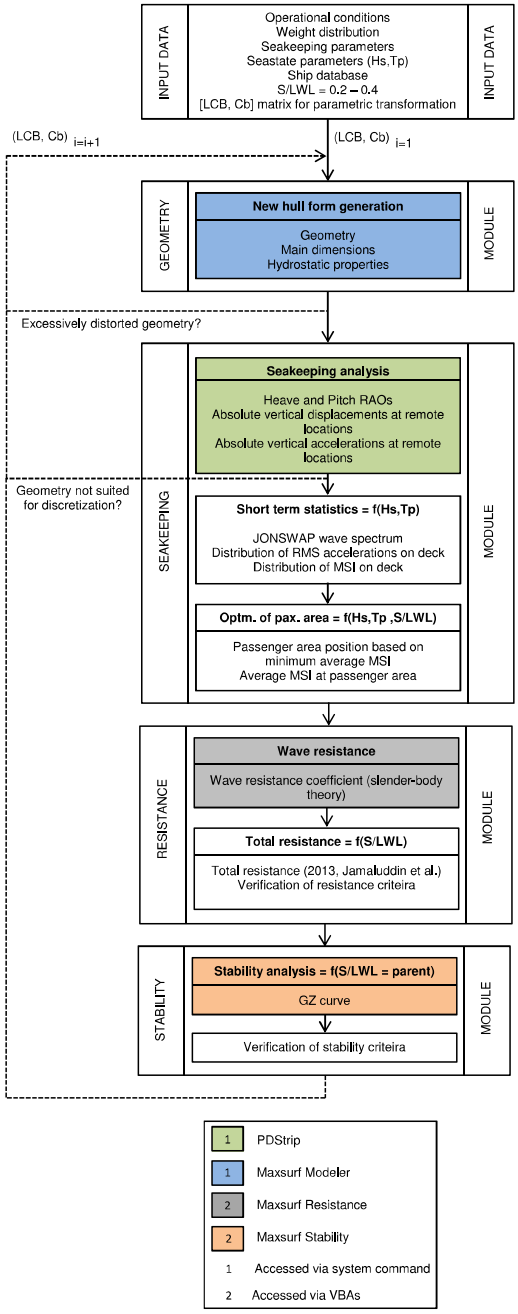

Figure 9: Flowchart of the MATLAB procedure that generates hull variations from the parent model and evaluates them in terms of seakeeping, resistance and stability

3.3. *Optimization results*

To present the optimization results, colour plots were used. The idea was to facilitate the visualisation of the gradient of the studied parameters as functions of LCB (measured with respect to $LPP/2$) and C_b, each pair representing a different generated model. Results are shown only for the case of the original horizontal clearance ratio $S/LWL = 0.2872$, Figure 10(a) for RMS vertical acceleration (in this case independent of S/LWL), Figure 10(b) for MSI and Figure 10(c) for total hull resistance R_T. Figure 10(d), which shows the percentage of models that satisfied the resistance criteria upon different horizontal clearance ratios, is presented as well, as it points out that for $S/LWL \leq 0.28$ there are no feasible solutions. Furthermore, as all models fulfilled the HSC code requirements, stability criteria did not affect the selection of the optimum solution and thus such results will not be shown.

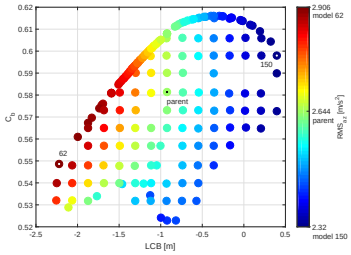

(a) RMS vertical acceleration responses at $x = 28.5$ m

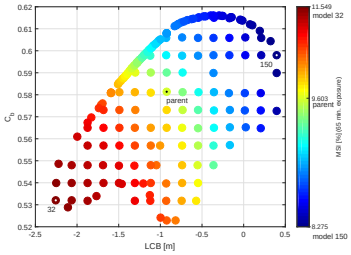

(b) Average MSI at passenger area for $S/LWL = 0.2872$

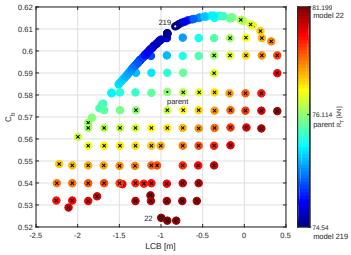

(c) Total hull resistance for $S/LWL = 0.2872$ (X marks models that failed to satisfy resistance criteria)

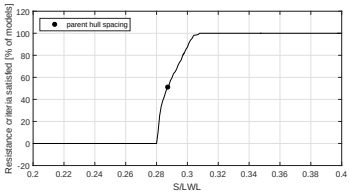

(d) Percentage of models that satisfy the resistance criteria as function of the horizontal clearance

Figure 10: Optimization results considering the most probable seastate at $V_s = 25$ knots ($H_{1/3}$ = 1-2 m, T_p = 11-13 s, prob = 14.51%) as function of (LCB, C_b)

The analysis of Figure 10(a) indicates that for the same C_b, an increase of LCB to an aft position will improve seakeeping performance, evaluated here in terms of RMS vertical accelerations. Regarding C_b, it seems that models with smaller values experience lower accelerations. However, the influence of block coefficient appears to be less significant, particularly for higher values of LCB. In any case, given that several other hull shape parameter are being varied as well, it is not possible to associate seakeeping improvements to single causes. In terms of motion sickness, similar results were observed in Figure 10(b) in the sense that a decrease of motion sickness is obtained by shifting LCB forward (for constant C_b values). However, it seems that decreasing C_b actually contributes for higher MSI values, an effect that, once again, becomes less significant as LCB increases. This has to do with the role of frequency on the MSI model. In fact, as pointed out by O'Hanlon and McCauley (1973), humans can apparently tolerate higher accelerations at higher frequencies without experiencing the same tendency towards motion sickness. Figure 7 indicates that above 0.16 Hz, where the frequency region experienced by all studied models is located, the lower $|f_e|$ is, the higher the experienced MSI for the same $|RMS_{az}|$ value. Furthermore, for a given frequency, MSI decreases with $|RMS_{az}|$. Since, as concluded before, decreasing C_b is not a very effective way to reduce $|RMS_{az}|$, the resulting reduction of $|f_e|$ leads to a higher incidence of motion sickness in that specific region of the model. In any case, model 150 seems to be the most suited in terms of seakeeping. From the point of view of ship resistance (Figure 10(c)), the optimum hull forms appear in regions of the figure that do not particularly favour the minimization of both RMS_{az} and MSI (Figures Figure 10(a) and 10(b)), suggesting incompatible trends.

3.4. *Selection of the optimum hull*

Figure 11, shows all generated models that satisfied the imposed criteria. Again, stability was not restrictive.

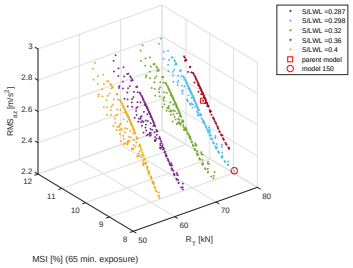

(a) 3-D representation of the family of possible solutions

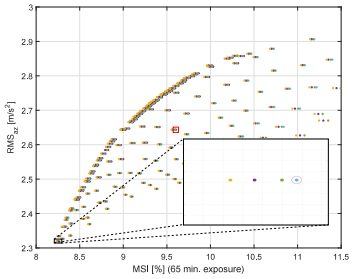

(b) Maximum RMS vertical acceleration response on deck as function of the average MSI at passenger area with detail view of the optimum region

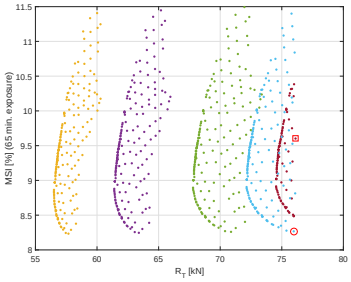

(c) Average MSI at passenger area as function of total hull resistance

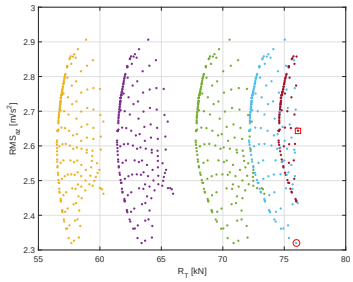

(d) Maximum RMS vertical acceleration response on deck as function of total hull resistance

Figure 11: Family of possible solutions considering the most probable seastate at $V_s = 25$ knots ($H_{1/3}$ = 1-2 m, T_p = 11-13 s, prob = 14.51%) with optimum hull model circled in red

Even though the objective functions only concern the minimization of RMS_{a_z} and MSI, a third axis with R_T was included. This provides information about the horizontal clearance that is being used, which in reality generates complete new sets of possible solutions, each assigned to a different colour. For simplicity, only 5 horizontal clearance ratios were displayed, ranging from the parent value to 0.4. It is interesting to note that, in fact, the lower the horizontal clearance ratio, the lower the number of possible solutions generated, which is in agreement with Figure 10(d). Again, it has been shown that model 150 is the most suited in terms of seakeeping. Although the horizontal clearance does not significantly affect MSI (Figures 11(b) and 11(c)), it is indeed a quite dominant parameter in terms of ship resistance (Figures 11(c) and 11(d)). In fact, the wider the catamaran hulls are set apart, the lower the total resistance which, of course, carries additional construction costs. Since seakeeping was the main focus of this dissertation, no efforts have been put into improving ship resistance and thus, model 150 was selected as optimum solution. Furthermore, $S/LWL = 0.298$ was the minimum horizontal clearance ratio that allowed its selection. In fact, due to the resistance criteria, as indicated by Figure 11, with lower S/LWL values, model 150 represents unsuitable solutions.

3.5. *Overview of model 150*

The main characteristics of both the parent model and the optimized model (model 150) are summarised in Table 8. Figure 12(a) shows the final rendered hull form and Figure 12 compares the body lines of both models. One of the things that immediately pops up is that model 150 is "bulgier" at the forward part, as a result of an increased LCB. Also, it seems that the parametric transformation of Lackenby affected the geometry of the bulbous bow significantly and it would have been interesting to use PDStrip to study alternative solutions for that region (e.g., a regular shaped bow without bulbous, an axe-bow or an inverted bow-type configuration).

Table 8: Main characteristics of the parent model and model 150

	Parent model	Model 150
LOA [m]	30	28.819
LWL [m]	28.386	28.387
BWL, demi-hull [m]	2.361	2.361
S [m]	8.152	8.459
BOA [m]	10.771	11.079
Deck area [m^2]	319.579	318.61
T (DWL) [m]	1.41	1.37
Δ [t]	112.600	112.513
KB [m]	0.868	0.883
KG [m]	1.5	1.5
LCB = LCG [m]	-0.926	0.399
C_b [-]	0.581	0.598
C_{wp} [-]	0.816	0.914
RMS$_{az}$ at $x = 28.5$ m [m/s^2]	2.644	2.320
Av. MSI at pax. area [%]	9.603	8.267
Pax. area [m^2]	50.73	50
Length of pax. area [m]	6.06	5.76
Free area aft [% of deck area]	10	11
Free area fwd. [% of deck area]	69	65
R_T [kN]	76.114	75.968

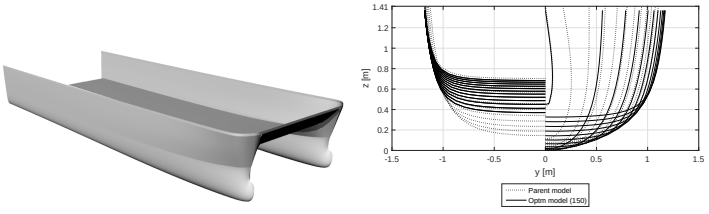

(a) Model 150 rendered in Rhinoceros (b) Underwater demi-hull body lines

Figure 12: Hull form comparison between the parent model and model 150

Figure 13 confirms that by optimizing for RMS vertical response accelerations at the bow, improvements in terms of heave and pitch RAOs have been achieved. Moving LCB forward by about 10% (as seen before, C_b has a weaker impact on heave and pitch motions) seems to have had a positive impact. In any case, as pointed out by Blok and Beukelman (1984), the verified increase of waterplane area (C_{wp} raised 12%) and BWL/DWL ratio probably influenced significantly these results as well. Thus, it is difficult to draw definite conclusions. Figure 13(a) indicates that at the resonance frequency (wavelengths of about 1.8-1.9LWL), model 150 experiences heaving amplitudes 16.5% smaller than the parent model. A decrease of the same order is observed for pitch at wavelengths of about $2LWL$ (Figure 13(b)). A small reduction of the total ship resistance was also achieved with the optimization.

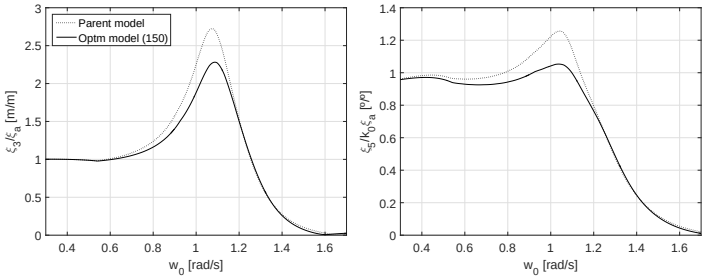

(a) Heave RAO as function of the wave frequency (b) Pitch RAO as function of the wave frequency

Figure 13: Comparison of heave and pitch RAOs at $V_s = 25$ knots

3.6. *Operability assessment of model 150 based on seakeeping criteria*

Finally, model 150 is analysed from the perspective of operability. An operability assessment considers human comfort criteria, being particularly vital in the design of passenger vessels. In Guedes Soares et al. (1995), the authors suggested that, due to linearity assumptions, the wave spectrum could be represented as the product of the wave spectrum in terms of the unitary significant wave height, $S_{\zeta 1}(\omega_e)$, and the square of the significant wave height $H_{1/3}$.

$$S_\zeta(\omega_e, H_{1/3}, T_p) = H_{1/3}^2 S_{\zeta 1}(\omega_e, T_p) \tag{20}$$

Using the previous result, equation (11) for the vertical response of the vessel at a remote location (x, y, z) can be rewritten as follows:

$$S_z(x, \omega_e, H_{1/3}, T_p) = |\xi_z(x, \omega_e)|^2 H_{1/3}^2 S_{\zeta 1}(\omega_e, T_p) \tag{21}$$

Recalling equation (12), given a seakeeping criterion defined in terms of RMS accelerations, $RMS_{a_z,criteria}$, the limiting significant wave height as function of the period (for this dissertation the peak period T_p is being considered) is given by equation (22).

$$H_{1/3}^{\lim}(T_p) = \frac{RMS_{a_z,criteria}}{RMS_{a_z,1}} \tag{22}$$

, where $RMS_{a_z,1}$ is the normalized root mean squared acceleration considering T_p.

The limiting criteria applied here are defined in the HSC (High Speed Craft) code [26] (*Chapter 4 Accommodation and Escape Measures, 4.3 Design acceleration*) and in the DNV GL rules for the classification of high speed crafts [13] (*Section 3 Structures, C3.3 Design Acceleration*). The first is associated with the maximum superimposed vertical accelerations at the centre of gravity of 1 g. The second relates with the longitudinal distribution of vertical accelerations. In both cases, the accelerations refer to average 1% highest accelerations rather than the RMS values, for which equation (23) from [24] has been applied. For this operability assessment, 25 knots (service speed) and 27 knots (90% of the maximum speed of 30 knots) have been the considered vessel speeds. Figure 14 shows the obtained limiting seastates for both op-

erational conditions.

$$az_{1/n} = \left[n\sqrt{2} \left[\frac{\sqrt{\ln n}}{n} + \sqrt{\pi} \left(\frac{1}{2} - erf\sqrt{2 \ln n} \right) \right] \right] RMS_{a_z} \quad (23)$$

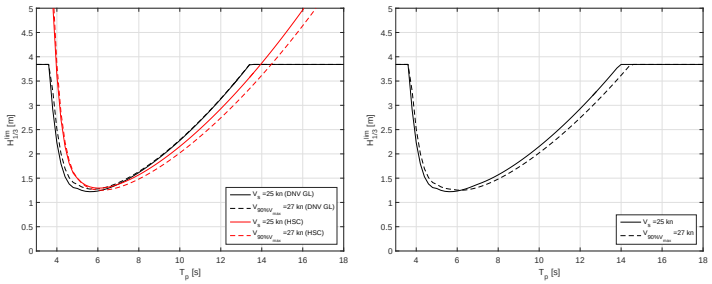

(a) Comparison of seakeeping criterion from DNV GL and HSC code for service speed and 90% of maximum speed

(b) Final limiting seastates for the operation of the fast crew supplier at service speed and 90% of maximum speed

Figure 14: Maximum allowed $H_{1/3}$ as function of the peak period based on criterion imposed by the classification societies

Finally, the operability index is defined as "the percentage of time during which the ship is operational" [18]. For that purpose, a scatter diagram can be used to sum up the probabilities of occurrence of the seastates upon which the catamaran is suited to operate according to Figure 14(b). However, the scatter diagram in Table 7, which presents wave data as function of ranges of significant wave height and peak period, does not present discretized enough data to allow for a reliable computation of the operability index. In any case, operability boundaries can be estimated based on the available information. From a conservative perspective, the fast crew supplier will be able to operate at the Alentejo basin only 52% of the time. In a more optimistic scenario, the author expects an operability index of 91%. Furthermore, it is likely that the effective operability is much closer to the upper boundary. Also, a decrease in operability is expected at higher speeds, given the more strict limitations.

4. Conclusions

Due to the widespread development of high-speed crafts and its use to transport passengers, the amount of research on the assessment and optimization of the seakeeping behaviour is vast. The present demands of the industry, which commonly resort to catamarans for this purpose, reinforce the relevance of the subject. A typical application of catamarans is as fast crew supply vessels, quite commonly found in the offshore industry. In this dissertation, a parent catamaran model provided by DAMEN Shipyards was optimized in terms of seakeeping to operate at 25 knots in the transport of 12 passengers to an offshore platform at the Alentejo basin, Portugal.

Despite a definite shift to three-dimensional seakeeping codes observed nowadays, the codes based on the strip-method still keep their value as they permit reasonably accurate and relatively fast predictions of ship motions in most situations. This motivated a comparison study of three codes based on the ordinary strip-theory (the open-source code PDStrip, the commercial code Maxsurf, and an in-house code earlier developed at CENTEC) which were applied to two ship forms: a fast mono-hull and a fast catamaran, for which experimental data from model testing were available. Heave and pitch motions upon head seas were the main focus of the analysis. PDStrip with transom terms seemed to be the most suited to use as seakeeping tool for the optimization of the fast crew supply catamaran.

With respect to the optimization of the catamaran, the optimum model was obtained by increasing C_b +3% and by shifting LCB forward by +10%. The resulting geometry also benefited from an increased waterplane area (+12% of C_{wp}) and a lower design draft (-2.8%). Results showed that increasing LCB decreases effectively the RMS vertical acceleration responses at the bow, while the influence of C_b is much less significant. In this regard, the optimum model allowed decreasing RMS accelerations by about 12%. In terms of motion sickness, the improvements were more subtle. With the optimum model, less 1.3% people experience motion sickness when compared to the parent model, which was also achieved by increasing the horizontal clearance by about 30 cm. An analysis of the RAOs of the optimum model allowed to conclude that at the resonance frequency, it experiences heaving amplitudes 16.5% smaller than the parent one. A decrease of the same order was observed for pitch. Regarding resistance, larger horizontal clearances decrease the interference effect and thus, lead to smaller total resistance forces. In order to comply with the resistance criteria (maximum allowed total ship resistance equal to the parent model), the horizontal clearance ratio of $S/LWL = 0.298$ was selected, which corresponds to the already referred decrease of 30 cm. These results allowed a decrease in consumption of less 1.88 kW of effective power at 25 knots. With respect to stability, only the parent horizontal clearance was evaluated, with which all models satisfied the criteria imposed by the classification societies. Given the small difference to the parent horizontal clearance, it is expected that no significant changes occur, although smaller horizontal clearances generally imply less transverse stability and an increase of the heeling angle at which the maximum GZ value occurs. Finally, an operability assessment of the optimized catamaran operating at two different speeds was carried out based on limiting seakeeping criteria imposed by the High Speed Craft (HSC) code and DNV-GL in terms of the average 1% highest accelerations. Estimates of the operability index indicated that from a quite conservative perspective, the fast crew supplier should be able to operate at the Alentejo basin only 52% of the time. In a more optimistic scenario, the author expects an operability index of 91% (the effective operability is probably much closer to the upper boundary).

References

[1] Ang, J. H., Goh, C., and Li, Y. (2015). Hull form design optimisation for improved efficiency and hydrodynamic performance of 'ship-shaped' offshore vessels. In *International Conference on Computer Applications in Shipbuilding (ICCAS) 2015*, Bremen, Germany. Royal Institution of Naval Architects, RINA.

[2] Bagheri, L., Ghassemi, H., and Dehghanian, A. (2014). Optimizing the seakeeping performance of ship hull forms using genetic algorithm. *The International Journal on Marine Navigation and Safety of Sea Transportation (TransNav)*, 8(1):49–57.

[3] Bai, K. J. and Yeung, R. W. (1974). Numerical solutions to free-surface flow problems. In *Proceedings of the 10th Symposium on Naval Hydrodynamics*, pages 609–647, Cambridge, Massachusetts, USA.

[4] Bentley Systems, Incorporated (2013). *Maxsurf Motions and Resistance, Windows Version 20, User Manuals.*

[5] Bentley Systems, Incorporated (2016). *Maxsurf Modeler and Stability, Windows Version 21, User Manuals.*

[6] Blok, J. J. and Beukelman, W. (1984). The high-speed displacement ship systematic series hull forms - seakeeping characteristics. *Trans-*

actions of the Society of Naval Architects and Marine Engineers, SNAME, 92:125–150.

[7] Carvalho, A. (2016). Análise do modelo de desenvolvimento de campos de hidrocarbonetos aplicado à bacia do alentejo. Master's thesis, Universidade de Aveiro.

[8] Castiglione, T., Stern, F., Bova, S., and Kandasamy, M. (2011). Numerical investigation of the seakeeping behavior of a catamaran advancing in regular head waves. *Ocean Engineering*, 38(16):1806–1822.

[9] Centeno, R., Fonseca, N., and Guedes Soares, C. (2000). Prediction of motions of catamarans accounting for viscous effects. *International shipbuilding Progress (ISP)*, 47(451):303–323.

[10] Chan, H. S. (1993). Prediction of motion and wave loads of twin-hull ships. *Marine Structures*, 6(1):75–102.

[11] Colwell, J. L. (1989). Human factors in the naval environment: a review of motion sickness and biodynamic problems. Technical Report DREA-TM-89-220, Defence Research Establishment Atlantic,, Dartmouth, Nova Scotia, Canada.

[12] Costa, M., Silva, R., and Vitorino, J. a. (2001). Contribuição para o estudo do clima de agitação marítima na costa portuguesa. In *2ª Jornadas Portuguesas de Engenharia Costeira e Portuária*, number 20, Sines, Portugal.

[13] DNV-GL (2012). *Rules for Classification and Construction, I Ship Technology, 3 Special Craft, 1 High Speed Craft*. DNV GL, 2012 edition.

[14] Dudson, E. and Rambech, H. J. (2003). Optimisation of the catamaran hull to minimise motions and maximise operability. In *Proceedings of the 7th International Conference on Fast Sea Transportation, FAST2003*, number P2003-7, Ischia, Italy.

[15] Faltinsen, O., Zhao, R., and Umeda, N. (1991). Numerical predictions of ship motions at high forward speed. *Philosophical Transactions: Physical Sciences and Engineering*, 334(1634):241–252.

[16] Fonseca, N. (2009). Apontamentos de dinâmica e hidrodinâmica do navio.

[17] Fonseca, N. and Guedes Soares, C. (1998). Time-domain analysis of large-amplitude vertical ship motions and wave loads. *Journal of Ship Research*, 42(2):39–153.

[18] Fonseca, N. and Guedes Soares, C. (2002). Sensitivity of the expected ships availability to different seakeeping criteria. In *Proceedings of 21st International Conference on Offshore Mechanics and Artic Engineering (OMAE'02)*, pages 595–603, Oslo, Norway.

[19] Frank, W. (1967). Oscillation of cylinders in or below the free surface of deep fluids. Technical Report 2375, Naval Ship Research and Development Centre, Washington DC, USA.

[20] Grigoropoulos, G. J. (2004). Hull form optimization for hydrodynamic performance. *Marine Technology*, 41(4):167–182.

[21] Guedes Soares, C., Fonseca, N., and Centeno, R. (1995). Seakeeping performance of fishing vessels in the portuguese economic zone. In *Proceedings of the International Conference on Seakeeping and Weather*, pages 1–10, London, England.

[22] Guedes Soares, C., Fonseca, N., Santos, P., and Maron, A. (1999). Model tests of the motions of a catamaran hull in waves. In *Proceedings of the International Conference on Hydrodynamics of High-Speed Craft*, pages 1–10, London, UK. Royal Institution of Naval Architects (RINA).

[23] Guo, Z., Ma, Q., and Hu, X. (2016). Seakeeping analysis of a wave-piercing catamaran using urans-based method. *International Journal of Offshore and Polar Engineering*, 26(1):48–56.

[24] Hoffman, D. and Karst, O. J. (1975). The theory of the rayleigh distribution and some of its applications. *Journal of Ship Research*, 19(3):12–191.

[25] Holloway, D. S. and Davis, M. R. (2006). Ship motion computations using a high froude number time domain trip theory. *Journal of Ship Research*, 50(1):15–30.

[26] IMO (2008). *International code of safety for high-speed craft (2000)*. IMO, Maritime Safety Committee (MSC), MSIS 34 (2008) edition.

[27] Jamaluddin, A., Utama, I. K. A. P., Widodo, B., and Molland, A. F. (2013). Experimental and numerical study of the resistance component interactions of catamarans. *Journal of Engineering for the Maritime Environment*, 227(1):51–60.

[28] Kapsenberg, G. K. (2005). Finding the hull form for given seakeeping characteristics. Technical report, MARIN, Wageningen, Netherlands.

[29] Kukner, A. and Sarioz, K. (1995). High speed hull form optimisation for seakeeping. *Advances in Engineering Software*, 22(3):179–189.

[30] Lee, C. M., Jones, H. D., and M, C. R. (1973). Prediction of motion and hydrodynamic loads of catamarans. *Marine Technology*, 10(4):392–405.

[31] Martins, J. M. (2015). Conferência: Pesquisa de petróleo em portugal. Entidade Nacional para o Mercado de Combustíveis (ENMC). Fundação Calouste Gulbenkian, Lisboa, Portugal.

[32] McCauley, M. E., Royal, J. W., Wylie, C. D., O'Hanlon, J. F., and Mackie, R. R. (1976). Motion sickness incidence: exploratory studies of habituation, pitch and roll, and the refinement of a mathematical model. Technical Report 1733-2, Office of Naval Research, Department of the Navy, Goleta, California, USA.

[33] Mousaviraad, S. M., Carrica, P. M., and Stern, F. (2010). Development and validation of harmonic wave group single-run procedure for rao with comparison to regular wave and transient wave group procedures using urans. *Ocean Engineering*, 37(8):653–666.

[34] Ogilvie, T. F. and Tuck, E. O. (1969). A rational strip theory of ship motions: Part i. Technical Report 013, Department Naval Architecture and Marine Engineering, College of Engineering, The University of Michigan, USA, Ann Arbor, Michigan, USA.

[35] O'Hanlon, J. F. and McCauley, M. E. (1973). Motion sickness incidence as a function of the frequency and acceleration of vertical sinusoidal motion. Technical Report 1733-1, Office of Naval Research, Department of the Navy, Goleta, California, USA.

[36] Ohkusu, M. and Takaki, M. (1971). On the motion of twin hull ship in waves. *Journal of the Society of Naval Architects of Japan*, 1971(129):29–40.

[37] Papanikolaou, A., Zaraphonitis, G., and Androulakakis, M. (1991). Preliminary design of a high-speed SWATH passenger/car ferry. *Marine technology*, 28(3):129–141.

[38] Piscopo, V. and Scamardella, A. (2015). The overall motion sickness incidence applied to catamarans. *International Journal of Naval Architecture and Ocean Engineering (IJNAOE)*, 7(4):655–669.

[39] Salvesen, N., Kerczek, C. H. V., Scragg, C. A., Cressy, C. P., and Melnhold, M. J. (1985). Hydro-numeric design of SWATH ships. *Transactions of the Society of Naval Architects and Marine Engineers, SNAME*, 93:325–346.

[40] Salvesen, N., Tuck, E. O., and Faltinsen, O. (1970). Ship motions and sea loads. In *Transactions of the Society of Naval Architects and Marine Engineers, SNAME*, volume 78, pages 250–287.

[41] Sarioz, K. (1993). *A hydrodynamic hull form design methodology for concept and preliminary design stage*. PhD thesis, University of Newcastle, Newcastle Upon Tyne, United Kingdom.

[42] Scamardella, A. and Piscopo, V. (2014). Passenger ship seakeeping optimization by the overall motion sickness incidence. *Ocean Engineering*, 76:86–97.

[43] Söding, H. (1993). A method for accurate force calculations in potential flow. *Ship Technology Research*, 40(4):176–189.

[44] Söding, H. and Bertram, V. (2009). Program PDSTRIP: public domain strip method. https://sourceforge.net/projects/pdstrip/.

[45] Söding, H., von Graefe, A., el Moctar, O., and Shigunov, V. (2012). Rankine source method for seakeeping predictions. In *Proceedings of the ASME 2012, 31st International Conference on Ocean, Offshore and Arctic Engineering*, pages 449–460, Rio de Janeiro, Brazil. American Society of Mechanical Engineers.

[46] Sun, H., Jiang, Y., Zhuang, J., and Zou, J. (2015). Numerical simulation of the longitudinal movement of a SSB catamaran in regular waves. In *2015 International Conference on Materials Engineering and Information Technology Applications (MEITA 2015)*, pages 530–535, Guilin, China. Atlantis Press.

[47] Triunfante Martins, P., Fonseca, N., and Guedes Soares, C. (2004). Comparação entre dados experimentais e numéricos do comportamento em ondas de um catamaran. In e V. Gonçalves de Brito, C. G. S., editor, *As Actividades Marítimas e a Engenharia*, pages 565–582. Edições Salamandra. ISBN: 972-689-229-5.

[48] Vernengo, G. and Bruzzone, D. (2016). Resistance and seakeeping numerical performance analyses of a semi-small waterplane area twin hull at medium to high speeds. *Journal of Marine Science and Application*, 15(1):1–7.